Measurement 74 (2015) 238–245

Contents lists available at ScienceDirect

Measurement

journal homepage: www.elsevier.com/locate/measurement

# Adaptative ECT system based on reconfigurable electronics

D.P. Morales, N. López-Ruiz, E. Castillo, A. García, A. Martínez-Olmos *

*Department of Electronics and Computer Technology, University of Granada, Granada 18071, Spain*

ARTICLE INFO

*Article history:*
Received 10 February 2015
Received in revised form 15 June 2015
Accepted 21 July 2015
Available online 28 July 2015

*Keywords:*
Electrical capacitance tomography
Reconfigurable
Programmable System on Chip
Smart-device
Android

ABSTRACT

In this work we present a novel scheme for the design of electrical capacitance tomography systems that is based on the use of reconfigurable electronics. The objective of this strategy is to generate an adaptable and portable prototype for the processing electronics, i.e., an instrument suitable to be easily transported and applied to different ECT sensors and scenarios with no need of hardware redesign. In order to show the benefits of this approach, a prototype of the processing electronics for the readings of the inter-electrode capacitance values has been implemented using a Programmable System on Chip (PSoC) that allows configuring both analog and digital blocks included in the design. The result is a compact and portable instrument that can work with any ECT sensor up to 8 electrodes. The measurements are sent through a wireless Bluetooth link to an external smart-device such as smartphone, where the permittivity distribution is reconstructed using a custom-developed Android application.



## 1. Introduction

Electrical Capacitance Tomography (ECT) is an imaging technique for the visualization of the instantaneous distribution in a multiphase flow formed by elements of different permittivity [1,2]. ECT is based on the measurement of the electrical capacitance between all the different electrode pairs surrounding a pipe when an electric field is applied. From these data, a reconstructed image of the permittivity distribution inside the vessel can be obtained [3,4]. In the typical architecture of an ECT system there are three well-differentiated parts: the sensor, formed by the measuring and guard electrodes, the acquisition electronics, which generates the data corresponding to the inter-electrode capacitances, and an external computer, where the image reconstruction is carried out. In the last years, numerous studies have been realized in order to optimize the response of these three parts [5–7]. The main advantage of ECT lies in its non-intrusive character, which makes this technique suitable for the imaging of environments that can be aggressive to the sensors placed within them, or that cannot be manipulated [8]. On the other hand, the main limitation for the use of this imaging technique is found in the capacitance measurement process itself, since the values of the capacitance changes to be registered can be below 10 fF [9]. This establishes a critical design issue of ECT systems, since they must be capable of measuring such weak variations on the standing capacitance between the different electrode pairs. Several design techniques have been developed in order to optimize the measurement electronics [9]. One approach consists of the replication of the sensing electronics for all the electrodes that form the sensor [10]. Nevertheless, this strategy leads to the development of complex systems of large dimensions. It is possible to integrate electronic boards on the pipe itself to reduce the stray capacitances induced by the cables that connect the electrodes to the circuitry [11,12].

This acquisition electronics must be finally connected to a computer where the image reconstruction is carried out and presented to the user. All these factors make these

* Corresponding author.
*E-mail address:* amartinez@ugr.es (A. Martínez-Olmos).

http://dx.doi.org/10.1016/j.measurement.2015.07.035
0263-2241/

systems expensive and difficult to manage. In addition, when a tomography system is designed, it is usually oriented to a particular application with fixed physical dimensions that determine the number and size of the electrodes and the capacitance range to be measured. Therefore, the electronics is developed and optimized for that application and cannot be applied to other without some redesigning.

In the recent years an alternative approach for the development of the electronics for sensor reading and interfacing has been proposed based on the use of reconfigurable devices [13–16]. This instrumentation is usually designed using Field-Programmable Gate Arrays (FPGA) as digital blocks and Field-Programmable Analog Arrays (FPAA) as analog blocks. The resulting systems offer versatile communication and flexible processing of the sensor's acquired signal, also providing the opportunity of analog conditioning for multiple and/or different sensors [17,18].

In this work, we propose an electrical capacitance tomography system based on reconfigurable electronics. In this system, the acquisition electronics is developed using a Programmable System on Chip (PSoC) that allows to implement both digital and analog blocks, including a microcontroller unit (MCU) and memory elements [19]. The PSoC is the whole electronic platform, and can be easily reconfigured to be adapted to different applications and measuring strategies, thus simplifying the complexity of reconfiguration in previous developed systems. The data obtained by this system are sent through a wireless communication based on Bluetooth technology to a smartphone or tablet, where the image reconstruction is carried out. For this purpose, an application for Android operating system has been developed and integrated in a smartphone in order to test the reconstruction image with real data.

## 2. System design

The aim of this work is the development of an ECT system using reconfigurable electronics. This strategy leads to a portable instrument for the measurement of the capacitance values arising between electrode pairs, suitable to be applied in different objectives, since the calibration and adaptation of the electronics to new scenarios is carried out by software, with no need of hardware redesign.

In order to demonstrate its feasibility, an 8-electrode sensor has been selected to be driven by the reconfigurable electronics. This number of electrodes provides enough sensibility for a broad set of applications [20–22]. The employed architecture follows a typical microcontrolled system scheme. All the electronics required for the measurement and processing of the capacitance data of the sensor have been implemented in a PSoC 5, which constitutes a single reconfigurable chip from Cypress Semiconductor Corporation (California, USA). This device offers a framework for full electronic system designs, which means that the entire signal path, from electrode excitation, analog signal acquisition, digitalization and finally data formatting and storage are performed within a single device. This fact simplifies the development of electronic instrumentation for sensor signal acquisition, which is the subject of this work.

The PSoC 5 presents a wide range of features, such as the presence of a Cortex-M3 Central Processing Unit (CPU); several types of memory elements including SRAM, flash, and EEPROM; digital systems that include configurable Universal Digital Blocks (UDBs) and specific function peripherals, such as USB; and analog subsystems that include configurable switched capacitor (SC) and continuous time (CT) blocks, up to 20-bit Delta Sigma converters, 8-bit digital-to-analog converters (DACs) that can be configured for 12-bit operation, more than one successive approximation register (SAR) analog-to-digital converter (ADC), comparators and programmable gain amplifiers (PGAs) [23]. All this system constitutes a powerful and complete toolbox for electronic design.

The above elements are organized around the MCU core and the designer selects how they are connected using programmable routing connections, all reconfigurable during run-time. The system is equipped with the necessary power resources that allow to power up the device from a single photovoltaic cell due to its DC–DC boost converter. These integrated modules perform a full system where the hardware is reduced when compared to other traditional designs based on microcontrollers. The analog resources allow the design of far different signal conditioning structures. In addition, the digital blocks enable the use of digital signal processing arrangements, along with pre-built communication components that may work in parallel, in standalone way or in conjunction with the MCU. Moreover, the digitalization of the signals and the analog conversion are driven by means of Direct Memory Access modules (DMA), thus releasing the MCU of these tasks. All the design is implemented with the PSoC Creator Integrated Design Environment (IDE), which allows concurrent hardware and application firmware design.

The ECT sensor designed in this application is built with 8 electrodes that iteratively act as source and sinks of a periodic voltage signal, usually a sinusoidal signal [9]. The objective of the reading electronics developed in the PSoC 5 is to measure and store the capacitance value among all the possible electrode pairs in the sensor. From these data, an image reconstruction showing the permittivity distribution inside the pipe on which the sensor is placed can be obtained through different reconstruction algorithms.

The signal path flow in the instrument is depicted in Fig. 1. The main tasks carried out by the system are: (i) generation of the excitation signal by means of a DAC and distribution to the electrode that acts as source in each moment through the multiplexers control algorithm; (ii) selection of the detection electrode and analog-to-digital conversion of the output signal of the capacitance transductor through the ADC module controlled by the DMA module, allowing an automatic memory storage of the measurements; (iii) processing of the measurements by the MCU firmware and their further transmission to an external device via a wireless Bluetooth link for image reconstruction. In the following, each of these tasks are explained with more detail.

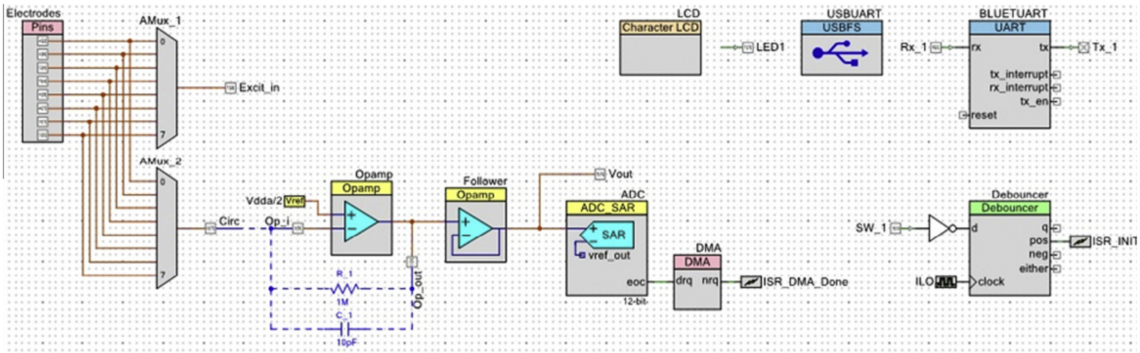


**Fig. 1.** Complete measuring electronics implemented in PSoC 5.

## 2.1. Source signal generation for electrode excitation

As it has been previously commented, the ECT technique requires that each electrode acts as signal source sequentially, and this also happens for the electrode that acts as sink. The developed instrument generates internally the excitation signal by means of a DAC controlled by a DMA module, as it is shown in Fig. 2, where a detail of the block implementation of the excitation electronics is presented. The DMA accesses to memory, where a set of 256 samples of a sinusoidal wave are previously stored, and sends the corresponding value to the 8-bit DAC in order to reproduce the original sinewave. This process generates a 60 kHz excitation wave with amplitude of 2.5 V. The selection of the source electrode is carried out by the microcontroller via the multiplexer module.

## 2.2. Capacitance measurement

For an 8-electrode sensor design there are 28 independent measurements that constitute the data set for a single image reconstruction [24]. The selection of the electrode to act as the sequential sink for each measurement is carried out by the MCU through a multiplexer module that drives the analog interface prior to the ADC conversion. Fig. 3 shows the analog arrangement for the inter-electrode capacitance measurement.

The analog circuit is configured as an AC-based capacitance transducer [9,25]. If the frequency of the injected signal at the source electrode $V_i$ is above the cut-off frequency

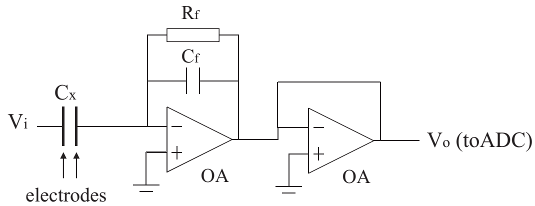


**Fig. 3.** Analog blocks arrangement for capacitance measuring.

introduced by the feedback net in the transducer stage formed by the resistor $R_f$ and the capacitor $C_f$, the output voltage amplitude $V_o$ is related to the unknown inter-electrode capacitance $C_x$ as [25]:

$$V_o = \frac{C_x}{C_f} V_i \quad (1)$$

In this particular case, the selected components for the feedback net of Fig. 3 set the cut-off frequency to 15.9 kHz. Therefore, taking into account that the reconstructed signal generated by the DAC corresponds to a 60 kHz sine-wave, from the measurements of the amplitude at the output of the analog block the values of the inter-electrode capacitance can be determined according to Eq. (1).

The design of the reading electronics using the architecture of the AC-based capacitance transducer provides relative immunity to stray capacitances induced by the wires that connect the electrodes to the electronic board, as it

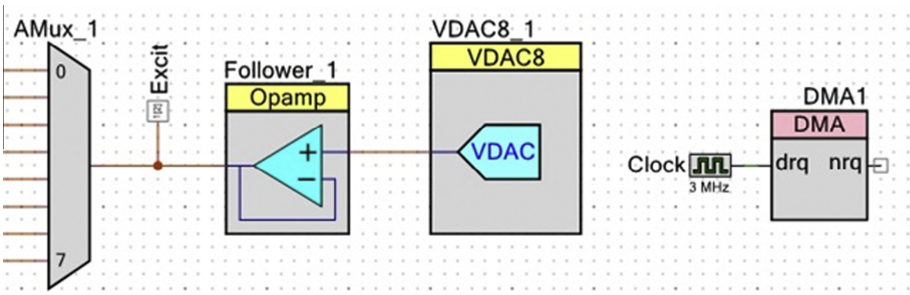


**Fig. 2.** Generation of the excitation signal.

is explained in [9]. Nevertheless, since the operational amplifiers are not ideal, the presence of these stray capacitances will affect the obtained values of the inter-electrode capacitance, and variations of these capacitances due to mechanical displacement of the cables, for example, may result in appreciable modification of the measured unknown capacitance. Therefore, a proper operation frequency must be selected in order to minimize the influence of the stray capacitance, as it is exposed in [25]. According to this work, the main effects of the stray capacitances will arise in two forms: (i) the introduction of a high frequency in the frequency-dependent gain of the operational amplifier used in the capacitance transducer pole that depends on the feedback capacitance, the value of the stray capacitance and the unity-gain bandwidth of the op-amp. In this case, the operational amplifiers implemented in the PSoC has a bandwidth of 6 MHz. Taking into account that the feedback capacitance is 10 pF, and assuming a typical value of 50 pF for the stray capacitances (cables are 50 cm long for the sensor of this design), the cut-off frequency induced by the stray capacitance is 1 MHz. Since the work frequency in this prototype is selected as 60 kHz, the effect of this high cut-off frequency should be negligible. The influence of the stray capacitance can be numerically evaluated by computing the relative stray-capacitance sensitivity which defined as the ratio of stray-capacitance sensitivity to unknown capacitance sensitivity [25]. In this case, and taking the worst case in which the inter-electrode capacitance is 1 pF, this relative sensitivity is $5.98 \cdot 10^{-5}$, which means that the variation in the output of the measurement circuit shown in Fig. 3 due to variations of the stray capacitance are indeed negligible; (ii) the current driven by the stray capacitance through the "on" resistance of the CMOS switches used in the multiplexer shown in Fig. 1. In the PSoC used in this work, these resistances can be as high as 200 Ω in the worst case, as pointed out in the datasheet. The combination of this resistance together with the stray capacitances has an influence on the output of the capacitance transducer as it is explained in [25]. This influence can be quantified by the relative stray-capacitance sensitivity, which in this case takes a value of $1.42 \cdot 10^{-5}$ for the worst case. Again, we can say that this effect has negligible influence on the output voltage of the transducer circuit, and we can directly take this value as a measurement of the unknown inter-electrode capacitance as it is expressed in Eq. (1).

The output voltage is digitalized by the analog-to-digital converter module, which is a 12-bit configurable SAR ADC, with a rate conversion of 640 ksps and an input range settled in the interval 0–5 V.

### 2.3. Data processing

The overall measurement process is controlled by the 32-bit ARM® Cortex™-M3 microprocessor core, which controls the multiplexer modules shown in Fig. 1 to select in each moment the source and detection electrodes, and also receives the data from the digitalization of the voltage measurement in the ADC. The amplitude of the output signal of the capacitance transducer is determined from the samples obtained from the analog-to-digital converter, using the standard IEEE-std-1057 [26]. The resulting data from a set of measurements are normalized and sent through a wireless communication via a Bluetooth link to an external PC or smart device such as smartphone, tablet, and smartwatch, where the image reconstruction is realized and presented to the user.

### 2.4. Prototype implementation

A fully-integrated prototype has been developed for the measuring and transmission of the capacitance values in an 8-electrode sensor, based on reconfigurable electronics. The system in presented in Fig. 4.

As it can be seen, it is a compact instrument which locates the PSoC 5 core implemented on a commercial board and provides communication with other modules. Two FPAAs have been integrated in the design for further applications, and they also provide modularity in order to expand the number of electrodes to be used in the sensor. For wireless transmission of the data, an embedded HC-05 Bluetooth module (Shenzhen Efortune Ltd., China) has been integrated in the PCB design. This module implements a Universal Asynchronous Receiver–Transmitter (UART) interface with programmable baud rate up to 460,800 bps. For data storage, a microSD memory card slot is also included in the instrument. The power supply of the system can be generated from 2 rechargeable batteries that provide 3 V for autonomous operation, or from an external power source connected to the prototype through a microUSB connector. This connector also allows controlling the instrument from a PC, which is appropriate for test and calibration purposes. With this aim, a Matlab® graphic user interface (GUI) has been developed. The physical connection to the sensor is carried out through 8 subminiature version A (SMA) connectors. The sensor used in this application is composed by 8 electrodes implemented on a PVC pipe with inner and outer diameters of 110 and 120 mm, respectively, using adhesive copper. Each electrode is 37 mm wide and 100 mm long, and they are separated by 5 mm one from another.

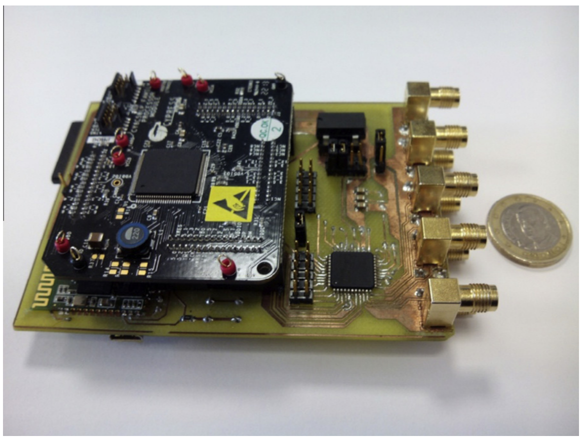

**Fig. 4.** PSoC-based integrated system for ECT.

### 2.5. Calibration

The described system has been calibrated using commercial capacitances that were adapted to the connecting cables to simulate the electrodes with different permittivity distributions between them. The resulting curve is presented in Fig. 5, where a plot of the obtained voltage amplitude at the output of the circuit of the Fig. 3 versus the measured capacitance is depicted, including error bars obtained as the standard deviation of the measurements for each point.

As it can be seen, the output voltage of the capacitance transducer and the measured capacitance are linearly related, as it is expressed by Eq. (1) with a high correlation factor $r^2 = 0.9931$. Nevertheless, an offset of −20.565 mV is present in the results, and it must be taken into account for the determination of the unknown capacitance $C_x$. From the slope of the linear fit, a sensitivity of 2.076 fF/mV is achieved. Having in consideration that the analog-to-digital converter has a resolution of 12 bits that corresponds to 1.23 mV resolution for an input range of 0–5 V, a resolution of 2.55 fF for the capacitance measuring electronics is obtained.

Although in Fig. 5 the minimum used value is about 100 fF, this is due to the effect of the stray capacitances which hamper the measurements of lower values of capacitances. However, as it can be observed, if only differences between contiguous capacitances values are taken into account, the range of variations allows to measure values from 10 to 1000 fF. Therefore, the measurement range of the instrument in this calibration procedure with the described configuration is 0.011 to 0.7 pF, which covers the range needed in ECT applications. Besides, if this measurement range is reduced for a concrete application, the resolution stated above can be easily improved.

For the measuring of very low capacitances (below 0.5 pF), the amplification of the output voltage $V_o$ is required. Using the technology here presented, that is the PSoC, this amplification can be carried out in two ways: firstly, by means of a pre-amplifier integrated in the SAR-ADC with programmable gain which allows to amplify the input signal before the sampling; secondly, it is possible to include programmable gain modules in the design, as it is done in the configuration of Fig. 6.

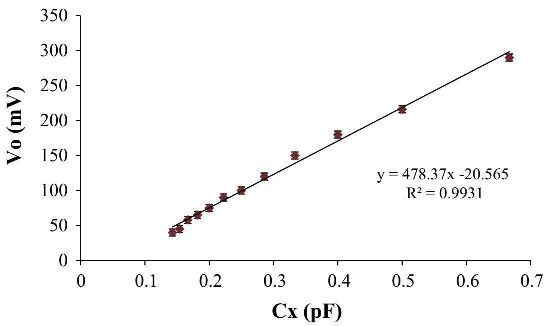


**Fig. 5.** Calibration curve.

In this figure, an alternative arrangement is presented that allows to combine the electrodes as segments in order to form electrodes with very high surface [16]. This case is here presented only to show the easy reconfiguration of the modules included in the PSoC to implement different measurement strategies with no need of hardware redesign.

## 3. Image reconstruction

The image reconstruction process in electrical capacitance tomography consists basically of the resolution of the inverse problem in ECT. This problem is aimed to generate the instantaneous permittivity distribution inside the vessel from the measured capacitance values, i.e., the resolution of the forward problem expressed in Eq. (2):

$$\lambda = \mathrm{S} \times \mathrm{G} \tag{2}$$

where $\lambda$ is the normalized capacitance vector, G is the normalized permittivity vector, and S is the sensitivity matrix, formed by all the sensitivity maps corresponding to the different electrode pairs in the sensor [27]. The direct solution of (2) could be expressed as $\mathrm{G} = \mathrm{S}^{-1} \times \lambda$. However, in general, the inverse of the sensitivity matrix does not exist, and the solution must be obtained as:

$$g = \widehat{\mathrm{S}} \times \lambda \tag{3}$$

where g is the approximation to the real solution and $\widehat{\mathrm{S}}$ is a modified sensitivity matrix that represents the inverse of S. In the simplest case, $\widehat{\mathrm{S}}$ is taken as the transposed matrix of S, which leads to the algorithm known as Linear Back-Projection (LBP) method:

$$g = \mathrm{S}^{\mathrm{T}} \times \lambda \tag{4}$$

This is the basis of the reconstruction algorithm used in this work. Nevertheless, this method is proven to generate fast but poor quality images. In order to improve the results, a technique for image fusion has been applied to this method. In this way, the method for combining the partial reconstruction images given by (4) is modified as:

$$g = \left(\mathrm{S}_1^{\mathrm{T}} \times \lambda_1\right) \cdot \left(\mathrm{S}_2^{\mathrm{T}} \times \lambda_2\right) \ldots \left(\mathrm{S}_n^{\mathrm{T}} \times \lambda_n\right) = \prod_{k=1}^{n} \left(\mathrm{S}_k^{\mathrm{T}} \times \lambda_k\right) \tag{5}$$

where $\mathrm{S}_i^{\mathrm{T}}$ and $\lambda_i$ are the transposed sensitivity matrix and normalized capacitance vector taken for the fixed source electrode *i*, respectively. This strategy has proved to highly improve the quality of the final reconstructed images with negligible time delay [28].

### 3.1. Android application

As it has been explained, the objective of this work is to develop a portable and adaptive system for electrical capacitance tomography, suitable to be applied on different sensors and scenarios, with no need of hardware redesign. The processing electronics presented here are aimed to drive the required signals in order to obtain the values of the inter-electrode capacitances in any ECT sensor. The final output of this prototype is the readings of these

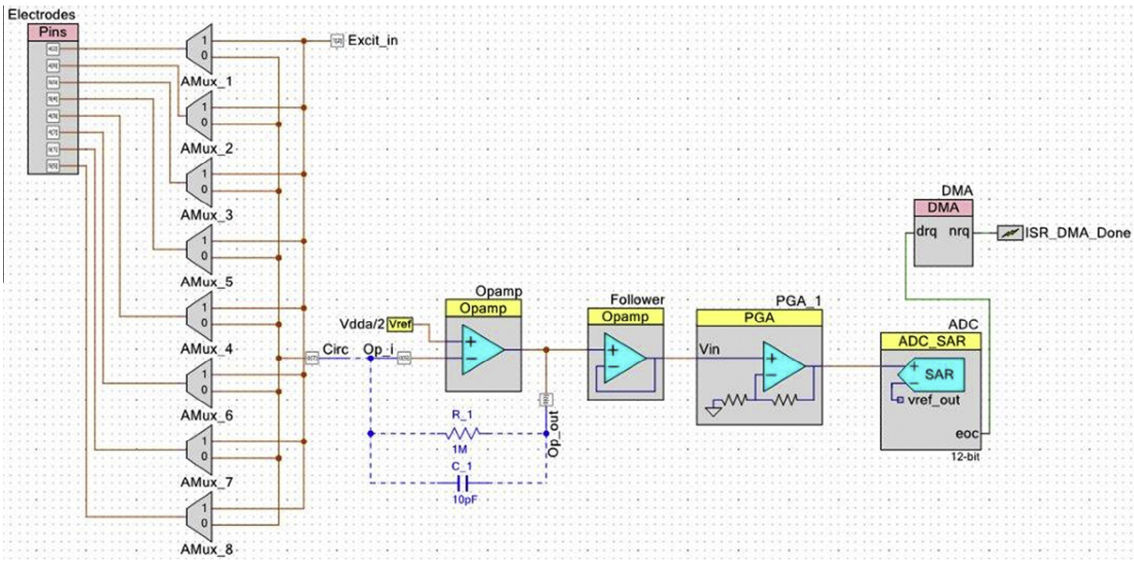


**Fig. 6.** Alternative configuration.

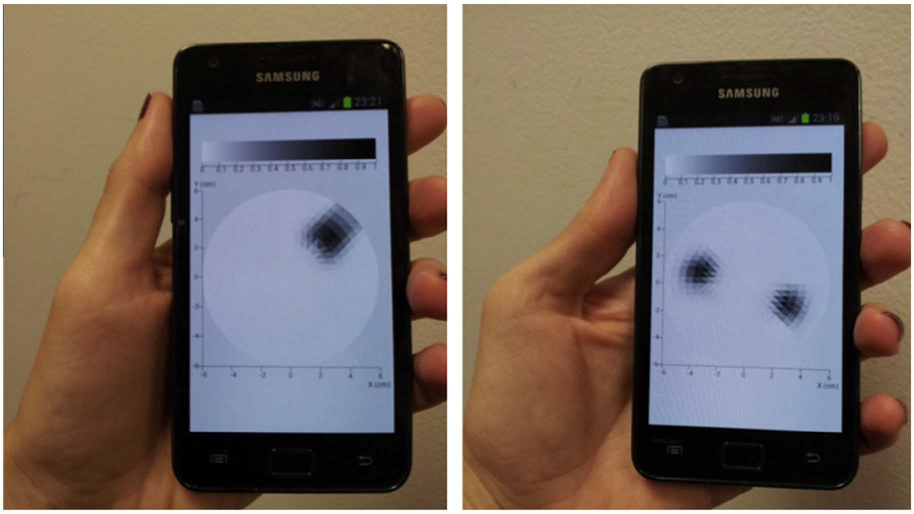


**Fig. 7.** Developed Android application used for image reconstruction.

capacitances that are used to reconstruct the permittivity distribution inside the pipe. Therefore, the presented instrument must be completed with a system for image reconstruction that also offers the same characteristics regarding portability and adaptability. With this objective, the classic personal computer that usually forms part of an ECT system for the implementation of the reconstruction algorithms and the visualization of the results [29] has been substituted by a smart-device such as smartphone, tablet, and smartwatch, that may be carried or even worn by the user. This device is programmed to receive the measurements of capacitance and to show in its display an instantaneous permittivity distribution. This strategy presents the main advantage that no specific system, such as a personal computer, is dedicated exclusively to this task, and therefore the required resources regarding cost and space are reduced. In addition, the ECT system installation is simplified, since the data transmission between the prototype described here for the measurement of the capacitances and the smart-device is based on a wireless Bluetooth link.

The above described technique for the image reconstruction based on the partial image fusion has been implemented in an application for Android operating system, since the market share for it is above the 80%, with only 7% for iOS from Apple Inc. (California, USA). Android can be used, as stated before, not only with smartphones, but also with tablets, and from last year with smartwatchs that receive notifications in the same way that a phone, wide opening the possibility of new designs for wearable technology. Therefore, the application has been developed to be adequate for several screen size and format characteristics.

For this work, a Samsung Galaxy SII smartphone from Samsung Electronics Co. (Seoul, South Korea) using Android 4.1.2 was chosen. This mobile phone has a display of 4.3″ with 640 × 480 pixels of resolution and dimensions of 125.3 × 66.1 × 49 mm, which are enough for the purpose here described (see Fig. 7).

The application receives via Bluetooth technology the normalized capacitance vector ($\lambda$), and following the reconstruction process detailed above, operates with matrices in order to calculate the final normalized permittivity vector ($g$) for representing the final image. The mobile phone has internally stored the sensitivity matrix needed and also the background to be coloured using the grey scale determined by the $g$ vector. That background composition depends on the number of electrodes used for each particular experiment and the number of vertex corresponding to that specific case. Since the $g$ vector is normalized, in order to obtain a grey intensity representation of the picture it is necessary to calculate an intensity vector between 0 and 255 values for each particular element of the drawn. Then, the application fills the corresponding element of the inner space with the corresponding grey colour (R, G and B coordinates use the same value to obtain a monochromatic representation). The results of the image reconstruction for two different measurements carried out using 8 electrodes are shown in Fig. 5.

This application can store sensitivity matrices for different number and size of electrodes, thus it is not exclusive for the presented case and it can be applied, as it is also the case with the acquisition electronics, for different sensors, resulting in a full adaptative ECT system.

## 4. Conclusions

In this work, a novel scheme for the design of ECT systems is proposed, based on the use of reconfigurable electronics. The purpose of this strategy is to obtain versatile and adaptative acquisition electronics for the determination of the inter-electrode capacitance values for any sensor and any application, with no need of hardware redesign and using smaller equipment. In order to validate this strategy a prototype has been developed, which is able to work with sensors up to 8 electrodes. A PSoC 5 has been used as the core of the instrument. This device counts with internal digital and analog blocks that allow a fast reconfiguration of the processing electronics for different sensors and scenarios. This instrument includes a Bluetooth module for wireless data transmission to an external device for storing or image reconstruction. In this case, the computation and visualization of the permittivity distribution from the capacitance measurements is carried out in a smartphone, where a custom developed Android application is running. This application receives the data through the Bluetooth link and generates the reconstruction using a modified Linear Back Projection algorithm for image fusion. The implemented system is a combination of a capacitance reading board and an image reconstruction application that results in a portable and flexible design suitable to be used for the visualization of dielectrics mixture flow under different conditions and requirements. For the measurement range here studied, from 0 to 0.7 pF, a sensitivity of 2.076 fF/mV and a resolution of 2.55 fF are achieved. These parameters can be improved if a reduced measurement range is considered.

## Acknowledgements

This work has been partially funded by Junta de Andalucía (University Professor and Researcher Training Program – FPDI grant) and by the CEI BIOTiC under project MPTIC10.

## References

[1] Z. Huang, B. Wang, H. Li, Application of electrical capacitance tomography to the void fraction measurement of two-phase flow, IEEE Trans. Instrum. Meas. 52 (2003) 7–12, http://dx.doi.org/10.1109/TIM.2003.809087.
[2] B.T. Hjertaker, S.A. Tjugum, E.A. Hammer, G.A. Johansen, Multimodality tomography for multiphase hydrocarbon flow measurements, IEEE Sens. J. 5 (2005) 153–160, http://dx.doi.org/10.1109/JSEN.2005.843903.
[3] H. Wegleiter, A. Fuchs, G. Holler, B. Kortschak, Analysis of hardware concepts for electrical capacitance tomography applications, IEEE Sens. 3 (2005) 688–691, http://dx.doi.org/10.1109/ICSENS.2005.1597792.
[4] C.G. Xie, S.M. Huang, B.S. Hoyle, R. Thorn, C. Lenn, D. Snowden, M.S. Beck, Electrical capacitance tomography for flow imaging - system model for development of image-reconstruction algorithms and design of primary sensors, IEE Proc. – G Circ. Dev. Syst. 139 (1992) 89–98.
[5] A. Martinez Olmos, J. Alberdi Primicia, J.L. Fernandez Marron, Simulation design of electrical capacitance tomography sensors, IET Sci. Meas. Technol. 1 (2007) 216–223, http://dx.doi.org/10.1049/iet-smt:20060108.
[6] J. Peng, P.K. Chan, Analysis of nonideal effects on a tomography-based switched-capacitor transducer, IEEE Sens. J. 7 (2007) 381–391, http://dx.doi.org/10.1109/JSEN.2006.890124.
[7] J. Lei, S. Liu, Z. Li, M. Sun, An image reconstruction algorithm based on the extended Tikhonov regularization method for electrical capacitance tomography, Measurement 42 (2009) 368–376, http://dx.doi.org/10.1016/j.measurement.2008.07.003.
[8] I. Ismail, J.C. Gamio, S.F.A. Burkhari, W.Q. Yang, Tomography for multi-phase flow measurement in the oil industry, Flow Meas. Instrum. 16 (2005) 145–155, http://dx.doi.org/10.1016/j.flowmeasinst.2005.02.017.
[9] W.Q. Yang, Hardware design of electrical capacitance tomography systems, Meas. Sci. Technol. 7 (1996) 225–232, http://dx.doi.org/10.1088/0957-0233/7/3/003.
[10] P. Brzeski, J. Mirkowski, T. Olszewski, A. Plaskowski, W. Smolik, R. Szabatin, Multichannel capacitance tomograph for dynamic process imaging, Opto-Electron. Rev. 11 (2003) 175–180.
[11] W.K. Harteveld, P.A. van Halderen, R.F. Mudde, C.M. van den Bleek, H.E.A. van den Akker, B. Scarlett, A fast active differentiator capacitance transducer for electrical capacitance tomography, in: 1st World Congress on Industrial Process Tomography. Buxton, Greater Manchester, April 14–17 1999.
[12] P. Williams, T. York. Evaluation of integrated electrodes for electrical capacitance tomography, in: 1st World Congress on Industrial Process Tomography. Buxton, Greater Manchester, April 14–17 1999.
[13] D.P. Morales, A. García, E. Castillo, M.A. Carvajal, L. Parrilla, A.J. Palma, An application of reconfigurable technologies for non-invasive fetal heart rate extraction, Med. Eng. Phys. 35 (2013) 1005–1014, http://dx.doi.org/10.1016/j.medengphy.2012.09.011.
[14] H. Yang, X. Wei, X. Liang, M. Su, X. Lu, A SoC and LED based reconfigurable subminiature spectrometer for hand-held measurement applications, Measurement 41 (2008) 44–54, http://dx.doi.org/10.1016/j.measurement.2006.11.022.

[15] A. Cabrini, L. Gobbi, D. Baderna, G. Torelli, A compact low-cost test equipment for thermal and electrical characterization of integrated circuits, Measurement 42 (2009) 281–289, http://dx.doi.org/10.1016/j.measurement.2008.06.011.
[16] A. Martínez, M.A. Carvajal, D.P. Morales, A. García, A.J. Palma, Development of a electrical capacitance tomography system using four rotating electrodes, Sens. Actuat. A 148 (2008) 366–375, http://dx.doi.org/10.1016/j.sna.2008.09.003.
[17] D.P. Morales, A. García, A. Martínez Olmos, J. Banqueri, A.J. Palma, Digital and analog reconfiguration techniques for rapid smart sensor system prototyping, Sens. Lett. 7 (2009) 1113–1118, http://dx.doi.org/10.1166/sl.2009.1244.
[18] H. Rabah, S. Poussier, S. Weber, Toward a generic on chip conditioning system for strain gage sensors, Measurement 39 (2006) 320–327, http://dx.doi.org/10.1016/j.measurement.2005.11.010.
[19] C.M. Huang, C.M. Wu, C.C. Yang, S.L. Chen, C.S. Chen, J.J. Wang, K.J. Lee, C.L. Wey, Programmable system-on-chip for silicon prototyping, IEEE Trans. Ind. Electron. 58 (2011) 830–838.
[20] C.G. Xie, A. Plaskowski, M.S. Beck, 8-electrode capacitance system for two-component flow identification. Part 1: tomographic flow imaging, IEE Proc. A – Sci. Meas. Technol. 136 (1989) 173–183.
[21] D. Yang, B. Zhou, C. Xu, S. Wan, Dense-phase pneumatic conveying under pressure in horizontal pipeline, Particuology 9 (2011) 432–440, http://dx.doi.org/10.1016/j.partic.2011.03.008.
[22] Y. Lia, M. Soleimani, Imaging conductive materials with high frequency electrical capacitance tomography, Measurement 46 (2013) 3355–3361, http://dx.doi.org/10.1016/j.measurement.2013.05.020.
[23] PSoC® 5LP: CY8C58LP Family Datasheet. Cypress Perform. Document Number: 001-84932 Rev. *G. December 8, 2014. http://www.cypress.com/?docID=49437.
[24] S.M. Huang, A.B. Plaskowski, C.G. Xie, M.S. Beck, Tomographic imaging of two-component flow using capacitance sensors, J. Phys. E: Sci. Instrum. 22 (1989) 173–177.
[25] J.C. Gamio, W.Q. Yang, A.L. Stott, Analysis of non-ideal characteristics of an ac-based capacitance transducer for tomography, Meas. Sci. Technol. 12 (2001) 1076–1082, http://dx.doi.org/10.1088/0957-0233/12/8/313.
[26] P. Händel, Properties of the IEEE-STD-1057 four-parameter sine wave fit algorithm, IEEE Trans. Instrum. Meas. 49 (2001) 1189–1193, http://dx.doi.org/10.1109/19.893254.
[27] H. Yan, F.Q. Shao, S. Wang, Fast calculation of sensitivity distributions in capacitance tomography sensors, Electron. Lett. 34 (1998) 1936–1937, http://dx.doi.org/10.1049/el:19981176.
[28] A. Martínez Olmos, G. Botella, E. Castillo, Diego P. Morales, J. Banqueri, A. García, A reconstruction method for electrical capacitance tomography based on image fusion techniques, Digital Signal Process. 22 (2012) 885–893, http://dx.doi.org/10.1016/j.dsp.2012.07.002.
[29] W. Yang, Design of electrical capacitance tomography sensors, Meas. Sci. Technol. 21 (2010) 042001.1–042001.13, http://dx.doi.org/10.1088/0957-0233/21/4/042001.